Disturbance Estimation based Robust FRI Tracking Control for Humanoid Robot

Devang Patwardhan
Student
IIT Madras
Chennai, India
patwardhandevang@gmail.com

Jaywant P. Kolhe
Scientist
R&DE(E), DRDO
Pune, India
jaywant.kolhe@gmail.com

S. E. Talole
Scientist
R&DE(E), DRDO
Pune, India
setalole@hotmail.com

doi: ttps://doi.org/10.37285/bsp.SACAD2025.43

***Abstract*—This paper presents a robust balance and walking control framework for humanoid robots combining Foot Rotation Indicator (FRI) tracking with disturbance estimation in a Linear Inverted Pendulum Model (LIPM) framework. As FRI point enables early detection of foot-ground instability, tracking FRI ensures global postural stability. An Uncertainty and Disturbance Estimator (UDE) compensates for the external disturbances acting on the robot. The effectiveness of the proposed robust control is demonstrated through simulations ensuring desired foot rotation indicator trajectory tracking performance in presence of external disturbances.**

Keywords—Humanoid, Balance & Control, Foot Rotation Indicator (FRI), Linear Inverted Pendulum Model (LIPM), Uncertainty and Disturbance Estimator (UDE)

I. INTRODUCTION

Achieving robust balance and locomotion remains one of the most critical and complex challenges in humanoid robotics. Despite significant progress over the past few decades, modelling inaccuracies, parametric uncertainties as well as disturbances arising from external forces compromise stability of the bipedal systems. Traditional methods relying solely on the Zero Moment Point (ZMP) criterion are effective in nominal conditions, however they tend to fall short in uneven, undulated terrain [1]. In this context, the Foot Rotation Indicator (FRI) offers a more sensitive and predictive measure of instability, providing early detection before the onset of foot tipping [2]. The primary motivation for this work stems from the inherent instability of bipedal walking and the limitations of conventional control strategies under real-world disturbances [3], [4]. While the LIPM has been extensively used due to its simplicity [5]–[7], it relies heavily on idealized assumptions that rarely hold true in practice [8], [9]. In such conditions, disturbances from uneven terrain, push recovery, or model uncertainties can lead to rapid loss of balance [10], [11]. Moreover, reliance on ZMP as a stability criterion can be problematic, as it often lags behind the actual instability event [1]. The FRI point, introduced as an alternative indicator, captures the rotational tendency of the foot and offers an earlier detection of loss of contact or tipping [2], [12]. The FRI point was proposed as a refinement over ZMP to detect incipient foot rotation or instability [12]. Unlike the ZMP, which may remain within the support polygon even as the foot begins to tip, the FRI anticipates this motion and migrates outside the contact area earlier, thus serving as a warning signal [1], [13]. By integrating this FRI into the control framework, we aim to develop a more proactive approach to balance the humanoid robot. Furthermore, incorporating disturbance estimation through the disturbance observer framework allows the controller to compensate for external and internal perturbations in real-time [11] ensuring robustness.

As stated earlier, ZMP-based control has widely been used in context of humanoid locomotion research since its inception [1]. Numerous studies have extended and optimized ZMP based walking, including pattern generation and preview control [5] and push recovery [9]–[11], [14]. Despite its success, ZMP inherently requires full foot contact and assumes a rigid, planar support surface, making it susceptible to modelling errors and locomoting through unstructured terrain [15]. To circumvent the complexity of full-body dynamics, researchers have leveraged simplified models such as the LIPM [5]– [7]. In [5], the authors formulated the preview control of ZMP trajectories using LIPM, and this approach became foundational for many biped control architectures [6], [8], [9], [16]. However, the simplifications in LIPM also introduced limitations when applied in the presence of disturbances [10], [11]. Several other techniques, such as centroidal momentum [3], [17], CoM height variation [18], or spring-loaded extensions [4], [15] have been reported, yet most remain limited by their assumptions of complete knowledge of the model and no disturbances acting on the system. The performance of these controllers severely degrade in presence of the external disturbance.

Various disturbance observer techniques have been reported in the literature wherein the disturbance is estimated and cancelled by augmenting the control law with the estimated disturbance. In [19] authors have proposed an extended state observer (ESO) for estimation of the system states as well external disturbances. In initial work of time delay control

(TDC) [20], disturbance is estimated utilising a function derived from the system dynamics and the nominal control is augmented with this estimate to cancel the effects of the external disturbance. A nonlinear disturbance observer (NDO) for estimation and compensation of the friction in two link manipulator is proposed in [21]. Next, [22] proposed a concept of uncertainty and disturbance estimator (UDE) and shown performance of the UDE estimator over the TDC in active disturbance rejection control. Building on this, various applications of UDE in disturbance estimation and control have been reported [23]–[27]. To this end various higher order filters have been proposed under UDE framework to estimate the fast-varying disturbances [28]–[30]. Applications of UDE in balance and walking control of humanoid robots have been reported in the literature, for example in [31], [32], the authors have proposed a UDE-based robust predictive controller for Center of Mass (CoM) tracking in humanoids using the Linear Inverted Pendulum Model (LIPM), showing strong disturbance rejection capability. In [33] UDE based robust joint servo control is proposed for biped walking; however, the outer balance and walking control is not designed.

The novelty of our work lies as follows: FRI is used not only as a diagnostic signal but also as a output feedback within the closed loop control framework [11]. By embedding the FRI into the LIPM dynamics and combining it with UDE, we allow the system to both predict postural instability and proactively cancel the unknown perturbations. This paper offers the following key contributions:(*i*) A disturbance-aware control framework for humanoid balance that incorporates FRI feedback with LIPM based simplified model of humanoid robot (*ii*) Application of the Uncertainty and Disturbance Estimator (UDE) to account for external disturbances ensuring robustness under real-world scenarios (*iii*) Simulation results validating the effectiveness of the proposed control law in maintaining balance against push disturbances. In essence, the paper presents a novel framework that combines FRIbased tracking with an Uncertainty and Disturbance Estimator (UDE) in a LIPM setting, enabling more resilient and responsive balance control for humanoids.

The remaining paper is organised as follows. Section II presents LIPM formulation as well as the relevance of FRI for LIPM model. UDE based robust state feedback control for FRI tracking has been proposed in section III. Numerical results of the proposed control scheme for LIPM model are presented in section IV. Lastly, section V provides the concluding remarks.

II. PROBLEM FORMULATION

Maintaining postural stability in humanoid locomotion relies heavily on monitoring moments at the support foot. A widely used stability criterion i.e. ZMP is defined as the point on the ground where the net moment of the ground reaction force (GRF) about the horizontal axes is zero [34], [35], i.e. $\tau_x = \tau_y = 0$, where τ_x, τ_x are the moments about the x and y axis respectively. While ZMP must lie inside the support polygon during balanced motion, it cannot indicate incipient foot rotation. To address this, Goswami [12] introduced the concept of FRI point, which identifies the point where the GRF must act to produce zero net moment about the foot. The distance between FRI and the nearest point of support polygon indicate the severity of the postural instability.

A. Foot Rotation Indicator (FRI)

Figure 1 illustrates a simplified single-link inverted pendulum model used for analyzing foot rotation during stance. The coordinate frame $\{\hat{e}_x, \hat{e}_y, \hat{e}_z\}$ defines the ground-fixed axes, with $\hat{e}_z$ oriented vertically upward. The pendulum of mass m is subjected to a ground reaction force f acting upward through the base, and its motion about the ground contact point is characterized by the Foot Rotation Indicator (FRI). The point of application of f determines the instantaneous rotation tendency at the foot. The angular rotation direction at the contact is shown by the curved arrow labeled "FRI."

The vectors $\vec{R}_1$, $\boldsymbol{\tau}_1$, $\vec{F}_{O_1}$, and $\vec{F}_{G_i}$ defined in Eqs. (1)–(3) are indicated in the figure. These represent, respectively, the net ground reaction force and ankle torque, the vector from the ankle origin to the FRI, and the force acting at the center of mass (CoM) of link i. The relationships established in Eqs. (1)–(3) form the foundation for the subsequent derivations in this section, linking the ankle moment balance to the FRI point location.

Now, let $\vec{R}_1$ and $\boldsymbol{\tau}_1$ be the net force and torque at the ankle joint, and $\vec{F}_{O_1}$ be the vector from ankle origin to the FRI.

$\vec{F}_{G_i}$ denotes the force at the CoM of link i, m_i its mass,

$\dot{\vec{H}}_{G_i}$

the rate of change of angular momentum about the CoM, and $m_i \vec{a}_i$ the inertial force from CoM acceleration. The general moment balance about the ankle is given as

$$\boldsymbol{\tau}_1 + \vec{F}_{O_1} \times \vec{R}_1 + \sum_{i=2}^{n} \vec{F}_{G_i} \times m_i \vec{g} = \sum_{i=2}^{n} \left(\dot{\vec{H}}_{G_i} + \vec{F}_{G_i} \times m_i \vec{a}_i \right) \tag{1}$$

Under quasi-static assumptions, i.e., by neglecting segmental inertia and acceleration, Eq. (1) simplifies to

$$\boldsymbol{\tau}_1 + \vec{F}_{O_1} \times \vec{R}_1 = \vec{F}_{G_1} \times m_1 \vec{g} \tag{2}$$

Here, i = 1 corresponds to modeling the entire body as a single-link pendulum, with the total mass concentrated at its CoM.

The FRI location in 2-D planar motion is given by

$$\vec{r}_{\mathrm{FRI}} = \vec{r}_{\mathrm{ZMP}} + \frac{\tau_{\mathrm{ankle}}}{F_z} \qquad (3)$$

where F_z is the vertical ground reaction force (GRF). As τ_{ankle} increases, the FRI shifts away from the Zero Moment Point (ZMP), potentially exiting the support polygon and signalling instability during stabilization and walking. This property of the FRI has been exploited in control systems to proactively counteract the effects of external disturbances.

This equation is used to obtain the desired FRI trajectory in Section II(D). Unlike the original definition of the FRI point, which is formulated in the inertial frame [12], we define the FRI point relative to the pendulum base. This prevents the trajectory from diverging during forward motion, ensuring that it remains bounded and thus more suitable for feedback control.

B. Linear Inverted Pendulum Model

Linear Inverted Pendulum Model (LIPM) [5] offers a reduced-order representation of humanoid robot for control applications. It assumes humanoid a point mass (CoM) located at a constant height Z_c, with massless, torque-free legs as shown in Fig. 1. The FRI representation in LIPM framework is shown in Fig. 2. Fig. 2 (a) represents the case where ankle torque $\tau_1 = 0$, while the angular velocity $\dot{\theta}_1 \neq 0$ and angular acceleration $\ddot{\theta}_1 \neq 0$, representing foot rotation without rolling, whereas Fig. 2 (b) represents the case where ankle torque $\tau_1 \neq 0$, $\dot{\theta}_1 = 0$, and $\ddot{\theta}_1 = 0$, representing static equilibrium with the FRI coinciding with the center of gravity (COG). Here, O_1 denotes the ankle joint, A and B are the heel and toe contact points defining the support polygon, and G_2 is the projection of the center of mass. γ is the angular deviation of the pendulum from the vertical, and C_1, C_2 indicate the limiting CoM positions during rotation. The shaded region beneath the foot represents the support area, with the FRI shifting within this region as a function of the applied ankle torque τ_1 and pendulum motion. The free body representation of FRI point is shown in Fig. 3.

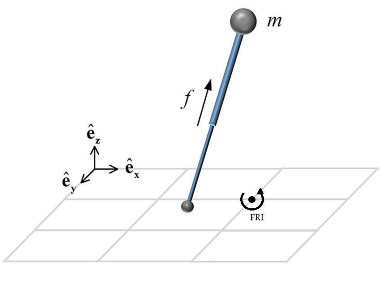

Fig. 1. Inverted pendulum model illustrating the Foot Rotation Indicator (FRI) with coordinate axes $\hat{e}_x, \hat{e}_y, \hat{e}_z$, applied force f, and mass m at the center of mass. The direction of foot rotation is shown by the curved arrow labeled "FRI."

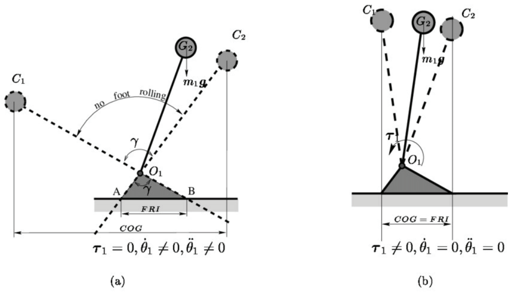

Fig. 2. Illustration of the Foot Rotation Indicator (FRI) under two different dynamic conditions. (a) case when ankle torque $\tau_1 = 0$ (b) case when $\tau_1 \neq 0$

The horizontal motion of the CoM is given as given in [36] is,

$$\begin{aligned} \ddot{x} &= \frac{g}{Z_c}(x - x_{ZMP}) = \frac{g}{Z_c}x + \frac{1}{mZ_c}u_x \\ \ddot{y} &= \frac{g}{Z_c}(y - y_{ZMP}) = \frac{g}{Z_c}y + \frac{1}{mZ_c}u_y \end{aligned} \qquad (4)$$

where g is the gravitational acceleration and x_{ZMP} and y_{ZMP} are the locations of ZMP in x,y plane respectively, serving both as a stability criterion and control input for CoM trajectory tracking.

C. Foot Rotation Indicator Point for LIPM

FRI point in the LIPM framework is derived by considering both the inertial effects of the CoM and the external torques acting at the ankle. Let us define the following variables,

- (x,y): CoM position in horizontal plane
- $\ddot{x}, \ddot{y}$: horizontal CoM acceleration
- m: mass of the robot
- u_x, u_y: ankle torques about x,y-axes respectively

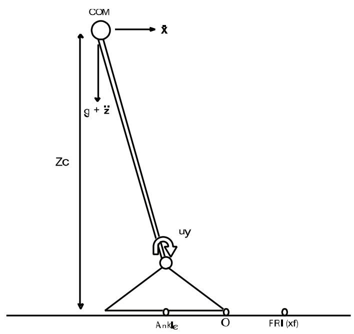

Fig. 3. Free-body representation used for deriving the FRI point in x-z plane The ground reaction force **R** generates a moment that balances gravitational and inertial moments about the ground.

To derive the location of the FRI point, a moment balance about ground has been considered. The ground reaction force R must counteract the inertial and gravitational forces and create a moment that cancels the ankle torque. The total moment about the origin O on the ground can be written as

$$\tau_{net} = m(x_f - x)(\ddot{z} + g) + Z_c m\ddot{x} - u_y = 0 \quad (5)$$

With CoM height constraint, $\ddot{z} = 0$,, and the moment about the y-axis is given by,

$$\tau_y = mg(x_f - x) + mZ_c\ddot{x} - u_y = 0 \quad (6)$$

Now, solving for FRI point i.e. x_f, y_f, one gets

$$\begin{aligned} x_f &= x - \frac{Z_c}{g}\ddot{x} + \frac{u_y}{mg} \\ y_f &= y - \frac{Z_c}{g}\ddot{y} + \frac{u_x}{mg} \end{aligned} \quad (7)$$

Not that (7) is equivalent to (3) proposing an alternative formulation of FRI.

D. Desired FRI Trajectory

The desired FRI point represents the location on the ground where the net horizontal moment vanishes. The horizontal dynamics of the LIPM is given by

$$\begin{aligned} \ddot{x} &= \frac{g}{Z_c}(x - x_{FRI}) \\ \ddot{y} &= \frac{g}{Z_c}(y - y_{FRI}) \end{aligned} \quad (8)$$

where $x(t)$, $y(t)$ are the horizontal CoM positions. Rearranging (8) one gets

$$\begin{aligned} x_{FRI} &= x - \frac{Z_c}{g}\ddot{x} \\ y_{FRI} &= y - \frac{Z_c}{g}\ddot{y} \end{aligned} \quad (9)$$

Eq. (9) is used to obtain the FRI point of the humanoid robot.

E. Desired CoM Acceleration Profile

During single support phase, the desired CoM acceleration trajectory is typically generated using a hyperbolic profile
symmetric about the midpoint $t = t_d$, let $\omega = \sqrt{g/Z_c}$ [16]. Then the desired CoM acceleration is given by

$$\begin{aligned} \ddot{x}(t) &= \omega^2(C_{x1}\cosh(\omega(t-t_d)) + C_{x2}\sinh(\omega(t-t_d))) \\ \ddot{y}(t) &= \omega^2(C_{y1}\cosh(\omega(t-t_d)) + C_{y2}\sinh(\omega(t-t_d))) \end{aligned} \quad (10)$$

Substituting (10) into (9) we get the desired FRI trajectory.

III. UDE BASED ROBUST STATE FEEDBACK CONTROLLER (SFC) FOR FRI TRACKING

This section presents a model based approach for regulating the FRI trajectory in humanoid robots. The model based controller is designed based on the LIPM dynamics of (4). The objective is to ensure stability and desired FRI trajectory tracking by appropriately generating the ankle torques. From (4) and (7), the LIPM dynamics is decoupled in terms of state variables (x, y), output (x_{FRI}, y_{FRI}) and control input (u_x, u_y), hence the control design and disturbance estimation for the dynamics of LIPM in x plane only is considered further.

A. SFC for FRI Tracking

Let the desired FRI position and velocity be denoted by $x_{FRI,des}$, $\dot{x}_{FRI,des}$ respectively, and the desired horizontal acceleration of the CoM is $\ddot{x}_{des}$. The FRI point using the LIPM relationship is computed as given by (7). The tracking error is defined as $e_{FRI,x} = x_{FRI,des} - x_{FRI}$ and $\dot{e}_{FRI,x} = \dot{x}_{FRI,des} - \dot{x}_{FRI}$. Now, Consider

$$u_x = \frac{1}{b}(u_{ax} + v_x) \quad (11)$$

SFC control for the LIPM dynamics of (4) is designed as

$$v_x = \ddot{x}_{des} + K_{dx}\dot{e}_{FRI,x} + K_{px}e_{FRI,x} \quad (12)$$

where $b = \frac{1}{mZ_c}$ and v_x is designed as the outer loop control given by (13)

$$v_x = \ddot{x}_{des} + K_{dx}\dot{e}_{FRI,x} + K_{px}e_{FRI,x} \quad (13)$$

The controller of (12) along with the outer loop controller of (13) is denoted as a state feedback controller (SFC). The gains of (13) need to choose properly to achieve desired tracking performance.

B. UDE based Robust SFC for FRI Tracking

Conventional feedback controllers may deliver degraded tracking performance due to model uncertainties and external disturbances. To compensate for such disturbances, the Uncertainty and Disturbance Estimator (UDE) framework was proposed [22]. Effectiveness of UDE based disturbance depends on the filter order and its frequency response. In general, higher-order UDEs are effective in compensating high-frequency disturbances.

The LIPM dynamics of (4) representing sagittal x-plane, in presence of the external disturbances d_x , is rewritten as

$$\ddot{x} = \frac{g}{Z_c}x + \frac{1}{mZ_c}u_x + d_x \quad (14)$$

The robust FRI tracking SFC control is obtained as

$$u_x = \frac{1}{b}(u_{ax} + v_x + u_{dx}) \quad (15)$$

where u_{dx} nullifies the disturbance and is written as

$$u_{dx} = -\hat{d}_x \quad (16)$$

Where $\hat{d}_x$ is estimation of the actual disturbance d_x. Rearranging (14), the true disturbance can be expressed as

$$d_x = \ddot{x} - u_{dx} + v_x \quad (17)$$

In UDE framework disturbance is estimated by passing the disturbance information through an appropriate filter. In this work a first-order low-pass filter [22] is used. Following (17) and following the methodology of [22], [32] a first-order filter is chosen as

$$G_f(s) = \frac{\hat{d}_x}{d_x} = \frac{1}{1+\tau_x s} \quad (18)$$

with $\tau_x > 0$ as the filter time constant. In time domain, the estimator of (18) satisfies

$$\tau_x \dot{\hat{d}}_x + \hat{d}_x = d_x \quad (19)$$

Substituting (17) into (19), one gets

$$\tau_x \dot{\hat{d}}_x + \hat{d}_x = \ddot{x} + \hat{d}_x + v_x \quad (20)$$

Integrating both the sides of (20), we obtain the disturbance estimate as

$$\hat{d}_x = \frac{1}{\tau_x}\dot{x} - \frac{1}{\tau_x}\int v_x \, dt \quad (21)$$

Substituting the disturbance estimation given by (21) into the control law of (15) we get UDE based Robust SFC control law.

IV. SIMULATION RESULTS

Numerical simulations are performed to test efficacy of the proposed robust FRI control law. The simulation data used for 3-LIPM for NAO humanoid [37], [38] is given in Table I. The reference FRI trajectories for the LIPM representing *NAO* humanoid are designed as given in Section II-D with the data given in Table I. The external disturbance $d_x = 2sin(t)$ and $d_y = 2cos(t)$ is injected in the system represented by (14). The control system specifications for the LIPM trajectory tracking are given in Table I. Next, the FRI controller gains k_1 and k_2 in (13) are chosen to satisfy the control system specifications. With this data, simulations are carried out for the proposed design of UDE based robust SFC control of (15) discussed in section III. The results of the FRI trajectory tracking of 3−D LIP are presented in Fig. 4 from where one can note that the FRI trajectory is being tracked satisfactorily despite of the presence of the external disturbance. Actual and estimated disturbances are shown in Fig. 5, it is evident that the UDE estimator of (21) could estimate the disturbance quite accurately.

TABLE I
SIMULATION PARAMETERS FOR 3−D LIPM MODEL OF NAO HUMANOID

Parameter	Definition	Value
m	mass of the robot	5.18kg
Z_c	Constrained height of CoM	0.32m
g	Gravity acceleration	9.81m/s^2
ts_x, ts_y	Desired settling times for FRI control	0.1s
ζ_x, ζ_y	damping ratios	1
τ_x, τ_y	filter time constants	0.05s
t_d	change time from DSP to SSP	0.1s
$[x(0), y(0)]$	initial position	[0;0]m
$[\dot{x}(0), \dot{y}(0)]$	initial velocity	[0;0]m/s

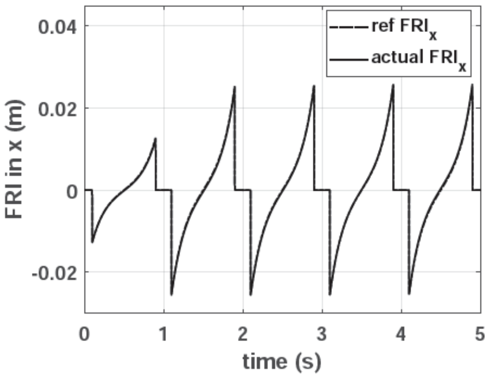

(a)

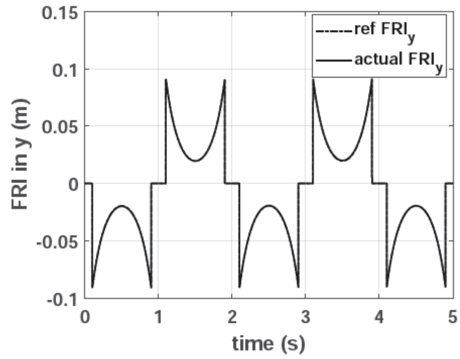

(b)

Fig. 4. FRI trajectory tracking performance for LIPM (a) x-axis (b) y-axis

V. CONCLUSIONS

In this work, UDE based robust SFC controller for FRI tracking of NAO humanoid for posture and walking is presented. From numerical simulations, it is evident that the FRI trajectory tracking performance of the UDE based robust SFC control is satisfactory thus addressing the issue of external disturbance.

(a)

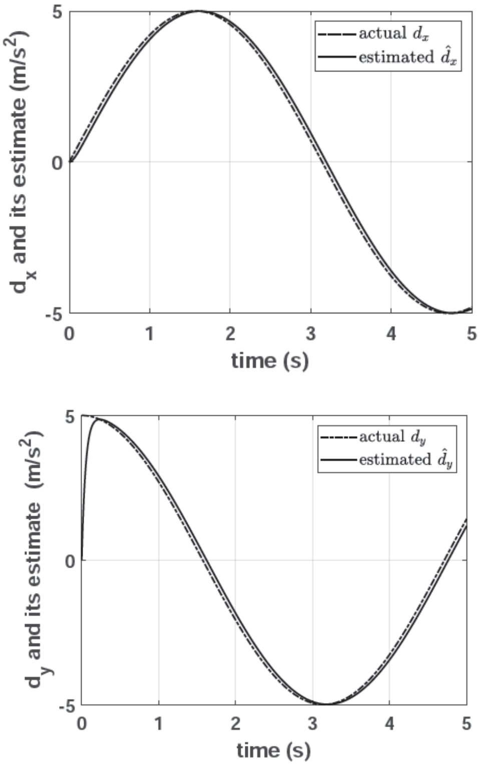

(b)

Fig. 5. Performance of disturbance estimation (a) d_x and its estimate (b) d_y and it's estimate

References

[1] M. Vutobratovic and B. Borovac, "Zero-moment point - thirty-five years of its life," *International Journal of Humanoid Robotics*, vol. 1, no. 1, pp. 157–173, 2004.

[2] J. Park and O. Khatib, "Contact consistent control framework for humanoid robots," in *IEEE International Conference on Robotics and Automation*, Orlando, FL, USA, 2006, pp. 1963–1969.

[3] M. Popovic, A. Hofmann, and H. Herr, "Angular momentum regulation during human walking: biomechanics and control," in *IEEE International Conference on Robotics and Automation, 2004. Proceedings. ICRA '04. 2004*, vol. 3, 2004, pp. 2405–2411.

[4] A. D. Kuo, "Stabilization of lateral motion in passive dynamic walking," *International Journal of Robotics Research*, vol. 18, no. 9, pp. 917–930, 1999.

[5] S. Kajita, F. Kanehiro, K. Kaneko, K. Fujiwara, K. Harada, K. Yokoi, and H. Hirukawa, "Biped walking pattern generation by using preview control of zero-moment point," in *IEEE International Conference in Robotics and Automation (ICRA*03*)*, 2003, pp. 1620–1626.

[6] T. Takenaka, T. Matsumoto, and T. Yoshiike, "Real time motion generation and control for biped robot 1st report: Walking gait pattern generation," in *IEEE/RSJ International Conference in Robotics and Automation*, 2009, pp. 1084–1091.

[7] S. Kajita, F. Kanehiro, K. Kaneko, K. Yokoi, and H. Hirukawa, "The 3-D linear inverted pendulum mode: a simple modeling for a biped walking pattern generation," in *Proceedings 2001 IEEE/RSJ International Conference on Intelligent Robots and Systems. Expanding the Societal Role of Robotics in the the Next Millennium (Cat. No.01CH37180)*, vol. 1, 2001, pp. 239–246.

[8] J. Englsberger, C. Ott, and A. Albu-Schaffer, "Three-dimensional¨ bipedal walking control using divergent component of motion," in *2013 IEEE/RSJ International Conference on Intelligent Robots and Systems*, 2013, pp. 2600–2607.

[9] J. Englsberger, C. Ott, M. Roa, A. Schaffer, and G. Hirzinger, "Bipedal walking control based on capture point dynamics," in *Proc. of IEEE/RSJ International Conference on Intelligent Robots and Systems*, San Francisco, CA, USA, 2011, pp. 4420–4427.

[10] B. Stephens, "Push recovery control for force-controlled humanoid robots," *Ph.D. Thesis, The Robotics Institute Carnegie Mellon University, USA*, 2011.

[11] B. J. Stephens and C. G. Atkeson, "Dynamic balance force control for compliant humanoid robots," in *2010 IEEE/RSJ International Conference on Intelligent Robots and Systems*, 2010, pp. 1248–1255.

[12] A. Goswami, "Postural stability of biped robots and the foot-rotation indicator (fri) point," *International Journal of Robotics Research*, vol. 18, no. 6, pp. 523–533, 1999.

[13] M. B. Popovic, A. Goswami, and H. Herr, "Ground reference points in legged locomotion: Definitions, biological trajectories and control implications," *The International Journal of Robotics Research*, vol. 24, no. 12, pp. 1013–1032, 2005.

[14] J. Englsberger, C. Ott, and A. Schaffer, "Three-dimensional bipedal walking control based on divergent component of motion," *IEEE Transactions on Robotics*, vol. 31, no. 2, pp. 355–368, 2018.

[15] Y. Zheng and J. Shen, "Gait synthesis for the SD-2 biped robot to climb sloping surface," *IEEE Transactions on Robotics and Automation*, vol. 6, no. 1, pp. 86–96, 1990.

[16] Y. Choi, D. Kim, Y. Oh, and B. You, "Posture/walking control for humanoid robot based on kinematic resolution of CoM Jacobian with embedded motion," *IEEE Transactions on Robotics*, vol. 23, pp. 1285– 1293, 2007.

[17] K. Kaneko, F. Kanehiro, S. Kajita, H. Hirukawa, T. Kawasaki, M. Hirata, K. Akachi, and T. Isozumi, "Humanoid robot HRP-2," in *IEEE International Conference on Robotics and Automation, 2004. Proceedings. ICRA '04. 2004*, vol. 2, 2004, pp. 1083–1090.

[18] T. Boaventura, C. Semini, J. Buchli, M. Frigerio, M. Focchi, and D. G. Caldwell, "Dynamic torque control of a hydraulic quadruped robot," in *2012 IEEE International Conference on Robotics and Automation*, 2012, pp. 1889–1894.

[19] Z. Gao, Y. Huang, and J. Han, "An alternative paradigm for control system design," in *Proc. of the 40th Conference on Decision and Control*, Orlando, Florida, USA, Dec 2001, pp. 4578–4585.

[20] K. Youcef-Toumi and O. Ito, "A time delay controller for systems with unknown dynamics," *Transactions of the ASME, Journal of Dynamic Systems, Measurement, and Control*, vol. 112, no. 1, pp. 133–142, 1990.

[21] W.-H. Chen, D. Ballance, P. Gawthrop, and J. O'Reilly, "A nonlinear disturbance observer for robotic manipulators," *IEEE Transactions on Industrial Electronics*, vol. 47, no. 4, pp. 932–938, 2000.

[22] Q. C. Zhong and D. Rees, "Control of uncertain LTI systems based on an uncertainty and disturbance estimator," *Transactions of the ASME, Journal of Dynamic Systems, Measurement, and Control*, vol. 126, no. 4, pp. 905–910, 2004.

[23] S. Talole, T. Chandar, and J. Kolhe, "Design and experimental validation of UDE based controller-observer structure for robust input–output linearisation," *International Journal of Control*, vol. 2184, pp. 969–984, 2011.

[24] A. Kuperman and Q. Zhong, "Robust control of uncertain nonlinear systems with state delays based on an uncertainty and disturbance estimator," *International Journal of Robust and Nonlinear Control*, vol. 21, pp. 79–92, 2011.

[25] B. Ren and Q. Zhong, "UDE-based robust control of variable-speed wind turbines," in *Proc. of the 39th Annual Conference of the IEEE Industrial Electronics Society (IECON)*, Vienna, Austria, 2013, pp. 3818–3823.

[26] J. Kolhe, M. Shaheed, T. Chandar, and S. Talole, "Robust control of robot manipulators based on uncertainty and disturbance estimation," *International Journal of Robust and Nonlinear Control*, vol. 23, pp. 104–122, 2013.

[27] J. Kolhe, A. Kodhanda, and M. Kuber, "Disturbance estimation based robust consensus of nonlinear multi-agent systems," in *Sixth Indian Control Conference (ICC)*, Hyderabad, India, 2019, pp. 86–91.

[28] T. Chandar and S. Talole, "Improving the performance of UDE-based controller using a new filter design," *Nonlinear Dynamics*, vol. 77, pp. 753–768, 2014.

[29] A. Kuperman, "Design of α-filter-based UDE controllers considering finite control bandwidth," *Nonlinear Dynamics*, vol. 81, pp. 411–416, 2015.

[30] A. Kodhanda and S. Talole, "Performance analysis of UDE based controllers employing various filters," *IFAC-PapersOnLine*, vol. 49, no. 1, pp. 83–88, 2016.

[31] J. Kolhe, S. Soumya, and S. Talole, "Disturbance estimation based robust center of mass tracking control of humanoid robot," *IFAC-PapersOnLine*, vol. 57, no. 1, pp. 315–320, March 2024.

[32] J. Kolhe, P. Uttam, S. Soumya, and S. Talole, "UDE based robust predictive control for CoM tracking of humanoid robot," in *Tenth Indian Control Conference (ICC)*, IISER, Bhopal, India, 2024, pp. 356–361.

[33] G. Cao, Q. Zhang, and Y. Zhou, "UDE-based robust walking control of a bipedal robot," in *Proceedings of 2021 Chinese Intelligent Automation Conference, Lecture Notes in Electrical Engineering, vol 801*. Springer, Singapore, 2021, pp. 38–46.

[34] M. Vutobratovic and J. Stepanenko, "On the stability of anthropomorphic systems," *Mathematical Biosciences*, vol. 15, pp. 1–37, 1972.

[35] S. Kajita, H. Hirukawa, K. Harada, and K. Yokoi, *Introduction to Humanoid Robotics (Springer Tracts in Advanced Robotics)*. Germany: Springer, 2014.

[36] S. Kajita and K. Tani, "Study of dynamic biped locomotion on rugged terrain-derivation and application of the linear inverted pendulum mode," in *IEEE International Conference in Robotics and Automation*, California, USA, 1991, pp. 1405–1411.

[37] "Nao- documentation," http://doc.aldebaran.com/2-4/family/robots/links robot.html, accessed: 2025-02-06.

[38] "Nao software 1.14.5 documentation," http://doc.aldebaran.com/114/family/robots/masses robot.html, accessed: 2025-02-06.